

Journal Pre-proof

Physicochemical, thermal and rheological properties of isolated Argentina quinoa starch.

María Paula López-Fernández, Silvio David Rodríguez, Leonardo Cristian Favre, Verónica María Busch, María del Pilar Buera



PII: S0023-6438(20)31102-6

DOI: <https://doi.org/10.1016/j.lwt.2020.110113>

Reference: YFSTL 110113

To appear in: *LWT - Food Science and Technology*

Received Date: 4 May 2020

Revised Date: 21 August 2020

Accepted Date: 24 August 2020

Please cite this article as: López-Fernández, Marí.Paula., Rodríguez, S.D., Favre, L.C., Busch, Veró.Marí., Pilar Buera, Marí.del., Physicochemical, thermal and rheological properties of isolated Argentina quinoa starch., *LWT - Food Science and Technology* (2020), doi: <https://doi.org/10.1016/j.lwt.2020.110113>.

This is a PDF file of an article that has undergone enhancements after acceptance, such as the addition of a cover page and metadata, and formatting for readability, but it is not yet the definitive version of record. This version will undergo additional copyediting, typesetting and review before it is published in its final form, but we are providing this version to give early visibility of the article. Please note that, during the production process, errors may be discovered which could affect the content, and all legal disclaimers that apply to the journal pertain.

© 2020 Published by Elsevier Ltd.

MPLF and PB contributed to the design and implementation of the research. MPLF, SDR, LCF and VMB carried out the experiment. MPLF wrote the manuscript with support from SDR, VMB and PB.

Journal Pre-proof

1 Physicochemical, thermal and rheological properties of isolated Argentina quinoa starch.

2
3 María Paula López-Fernández^{1,2*}, Silvio David Rodríguez^{1,2}, Leonardo Cristian Favre^{3,4}, Verónica María Busch^{3,4}, María
4 del Pilar Buera^{3,4,*}.

5 ¹Universidad de Buenos Aires, Facultad de Ciencias Exactas y Naturales, Departamento de Biodiversidad y Biología
6 Experimental, Intendente Güiraldes 2160, Ciudad Universitaria, C1428EGA, Buenos Aires, Argentina

7 ²CONICET-Universidad de Buenos Aires. Instituto de Biodiversidad y Biología Experimental (IBBEA)-Buenos Aires,
8 Argentina

9 ³Universidad de Buenos Aires, Facultad de Ciencias Exactas y Naturales, Departamentos de Industrias y Departamento
10 de Química Orgánica. Intendente Güiraldes 2160, Ciudad Universitaria, C1428EGA, Buenos Aires, Argentina.

11 ⁴CONICET - Universidad de Buenos Aires, Instituto de Tecnología de Alimentos y Procesos Químicos (ITAPROQ).
12 Intendente Güiraldes 2160, Ciudad Universitaria, C1428EGA, Buenos Aires, Argentina.

13 *Corresponding author

14 E-mail address: mapaula.lf@gmail.com, mpaula@bg.fcen.uba.ar

ABSTRACT

The aim of the present study was to evaluate the physicochemical, thermal and pasting properties of the starch of six quinoa genotypes native to the northwest of Argentina. The genotypes belonging to two genotype groups, highlands and dry valley, were grown in Jujuy, Argentina. Significant differences among genotypes were observed ($P < 0.05$) in amylose content, swelling power, water-binding capacity, thermal and pasting properties. In the different genotypes, the starch was characterized by a typical A-type X-ray diffraction pattern, with relative crystallinity ranging between 26.1 and 28.5%. Granule-bound starch synthase (GBSS), which is the single enzyme responsible for amylose biosynthesis, was also identified, with the 67- and 58-kDa quinoa polypeptides corresponding to the full-length and mature GBSS proteins. Studies of the pasting properties showed that the starch of the genotypes from the highlands had lower peak viscosity and lower breakdown parameter than that of the genotypes from the dry valleys. The results showed that the genotypic background and the environment influence the pasting curves. The novel findings discussed in this study constitute a starting point for research focusing on incorporating innovative technologies in the food and biomaterials industry.

Keywords: starch; quinoa; amylose; pseudocereals; genotype; DSC

List of Acronyms

AC = Amylose content

AAM = Apparent amylose

BD = Breakdown

BR = Setback ratio

Con A = Concanavalin A

CPV = Cool paste viscosity

DR = Degree of retrogradation

GBSS = Granule bound starch synthase

HPV = Hot paste viscosity

PCA = Principal component analysis

PKT = Peak temperature

PT = Pasting temperature

PV = Peak viscosity

S = Solubility

SB = Setback

48 ~~or Swelling power~~

49 ~~SR – Stability ratio~~

50 ~~WBC – Water binding capacity~~

51

52 1. INTRODUCTION

53

54 Starch, which is a renewable biopolymer, is the most common carbohydrate in the human diet. Starch is constituted by
55 two different glucose polymers: amylose and amylopectin. Amylose is a mainly linear polymer consisting of long chains
56 of α 1,4-linked glucose units, whereas amylopectin is a branched polymer in which linear chains of α 1,4-linked glucoses
57 are joined together by α 1,6 linkages (Smith, 2001). Starch synthesis is achieved through the coordinated interactions of
58 several biosynthetic enzymes, including: ADP-Glc pyrophosphorylases, starch synthases, starch branching enzymes
59 and starch debranching enzymes. Starch synthases can be divided into soluble starch synthases and granule-bound
60 starch synthases (GBSS) (Bahaji et al., 2014). In wheat, genetic analyses have indicated that amylose synthesis is
61 strictly dependent upon GBSS and does not specifically require any of the four starch synthases (Zi et al., 2018). G. Li &
62 Zhu, (2018a) reported that amylose content and amylopectin fine structure greatly influence the physicochemical
63 properties of starch, thus affecting grain and flour quality. Among the genera of the family Poaceae, the morphological
64 characteristics and composition of storage starch are known to vary considerably. In rice, barley, sorghum, and wheat,
65 this variation among genotypes has been shown to lead to considerable differences in the nutritional and industrial
66 properties of starch (Kong, Zhu, Sui, & Bao, 2015; Singh, Singh, Kaur, Singh Sodhi, & Singh Gill, 2003; Wani et al.,
67 2012). Quinoa (*Chenopodium quinoa* Willd.), which is a grain crop from the Andes region of South America belonging to
68 the family Amaranthaceae, has been cultivated for the last 7000 years and is well adapted to extreme environmental
69 conditions such as high altitude, low annual precipitation, high soil salinity and freezing temperatures. In the quinoa
70 grain, the main storage compound is starch, which accounts for 65–70% of its final dry weight and is synthesized in
71 perisperm cells during seed development, for 14 days after fertilization (López-Fernández & Maldonado, 2013). It is
72 important to highlight that the perisperm resembles the cereal starchy endosperm both morphologically and functionally
73 (Burrieza, López-Fernández, & Maldonado, 2014).

74 In the northwest of Argentina, Andean farmers sow quinoa in a wide range of altitudes, temperatures and rainfall. Native
75 quinoa crops are found from the western arid highlands area, passing through the dry valleys of the Quebrada de
76 Humahuaca and the Valles Calchaquies to the eastern Cordillera. Highland and valley quinoa genotypes show

77 differences in the grain number and weight and in their sensitivity to temperature and photoperiod (Curti, de la Vega,
78 Andrade, Bramardi, & Bertero, 2014).

79 Studies on new natural starches are crucial to find their best use and to increase the utilization of starchy flours (Jan,
80 Panesar, Rana, & Singh, 2017). Thus, screening the quinoa genotypes from northwestern Argentina will benefit the
81 identification of quinoa grains with different functional and compositional properties. So far, several studies have
82 examined the physicochemical, thermal (G. Li, Wang, & Zhu, 2016; Lindeboom, Chang, Falk, & Tyler, 2005; Steffolani,
83 León, & Pérez, 2013) and rheological properties of starch in different genotypes of quinoa (Jan et al., 2017; G. Li & Zhu,
84 2018b), but, to our knowledge, none has reported evidence about the influence of the genotype origin on its
85 physicochemical, thermal and pasting properties.

86 Understanding the impact of the agro-climatic conditions and genotype origin on the properties of quinoa starch is
87 strategic for food security and can facilitate the development of value-added utilizations. Thus, the aim of this work was
88 to isolate and characterize starch from six quinoa genotypes from two different ecological areas of northwestern
89 Argentina: the highlands and the dry valley. The relationship between the genotype origin and the variability in functional
90 properties, including swelling power (SP), solubility (S), water-binding capacity (WBC), pasting characteristics, thermal
91 transition temperatures, and amylose content were here evaluated. Due to the importance of the amylose pathway in
92 altering the physicochemical properties in the starch biosynthesis, the GBSS accumulation pattern was also evaluated.

93

94 **2. MATERIALS AND METHODS**

95 **2.1. Genotypes**

96 Quinoa (*Chenopodium quinoa* Willd.) genotypes from the northwest region of Argentina were studied. Genotypes,
97 provided by the National Institute of Agricultural Technology (INTA- Abra Pampa, Argentina), are the result of the 5-year
98 mass selection of the accessions CHEN 182, CHEN 252, CHEN 435, CHEN 420, CHEN 426 and INTA-Hornillos,
99 sheltered in the Germplasm Bank. The genotypes were from different ecological areas: dry valleys and highlands, of the
100 northwestern Argentina as described in (Curti et al., 2014)(Table 1). Quinoa grains were collected at Estación
101 Experimental Agropecuaria Abra Pampa Hornillos –Instituto Nacional de Tecnología Agropecuaria-INTA, (22,83° S,
102 65,85° O; 3484 m s.n.m.) in April 2016. The highland genotypes were harvested at 90-110 days after sowing whereas
103 dry valley genotypes were harvested 130-140 days after sowing (Curti et al., 2014). Experiments reported here were
104 repeated at least three times.

105

106

107

2.2. Starch isolation

108

109

110

111

112

113

114

Quinoa grains (100 g) were passed through a laboratory rice mill Suzuki (MT-95, Suzuki Co, São Paulo, Brazil) to remove the pericarp and the embryo. Starch was isolated according to Jan *et al.*, (2017) with slight modifications by steeping milled quinoa grains (mostly perisperm) in 0.25 % aqueous NaOH solution (pH 12.6) and kept at 4 °C for 24h. Next, the samples were grinded in a Waring® blender for 1 min, the slurry was screened over 60 and 200 Tyler mesh, and centrifuged for 10 min at 3,500 ×g. Finally, the pellet was dispersed in distilled water and centrifuged, up to neutrality. The starch was freeze-dried (Heto Holten A/S, cooling trap model CT 110 freeze-dryer, Heto Lab Equipment, Denmark) and stored in hermetic sealed vials at 25 °C until used.

115

2.3. Isolation of granule- bound starch proteins

116

117

118

119

120

121

122

123

124

Quinoa granule- bound starch proteins were isolated according to Lindeboom *et al.*, (2005) with slight modifications. Briefly, dried starch (20 mg) was dispersed in 250 µl of extraction buffer [55 mM Tris-HCl, pH 6.8; 2.3 % (w/v) SDS; 5 % (v/v) β-mercaptoethanol; 10 % (v/v) glycerol; 0.0005 % (w/v) bromophenol blue], and boiled (100 °C) for 5 min. The suspension was centrifuged at 15,000 × g for 10 min at 4 °C. The supernatant containing the granule- bound starch proteins was decanted from the gelatinized starch pellet and 7 µl of the resulting supernatant were electrophoresed using a Mini-Protean II (Bio-Rad Laboratories, Hercules, CA, USA). The extracts fractionated on SDS-PAGE gels were stained by Coomassie Brilliant Blue staining (0.1 % Coomassie R250, 10 % acetic acid, 40 % methanol) for 1 h at room temperature, and destained by several rinses with hot distilled water until proper contrast was achieved. The gels were photographed using G:Box GeneSnap software from Syngene.

125

2.4. Western blot and signal quantification analysis

126

127

128

129

130

131

132

133

The isolated protein extracts (7 µl), obtained as described above in 2.3 were electrophoresed using a Mini-Protean II (Bio-Rad Laboratories, Hercules, CA, USA). The protein extracts were separately analyzed on a 10% SDS -PAGE and electrotransferred at 4°C onto a nitrocellulose membrane (Hybond Amersham Pharmacia Biotech, Freiburg, Germany) at 100 V for 1 h using a MiniTrans-Blot electrophoretic transfer cell (Bio-Rad Laboratories, Hercules, CA, USA). Additionally, prior to immunoblotting, membranes were stained with 0.1 % (w/v) Ponceau S and 5 % (v/v) acetic acid to ensure equal loading of protein. The membranes were immersed in 3 % BSA blocking solution in TTBS (50 mM Tris-HCl, 150 mM NaCl, pH 8, 0.05 % Tween-20) overnight at 4 °C with gentle shaking. The blots were subjected to three 15-

134 min rinses in TTBS solution and were incubated with primary antibody raised against rice G6P1 (Fujita *et al.*, 2000)
135 diluted 1:1000 in blocking solution for 2 h on an orbital shaker at room temperature. Blots were then incubated with
136 secondary antibody, Donkey Anti-Rabbit IgG (Thermo Fisher Scientific Pierce, MA, USA.) conjugated to alkaline
137 phosphatase diluted 1:5000 in blocking buffer for 1 hour at room temperature and subjected to five 15-min rinses in
138 TTBS solution. Immunoreactive bands were detected with the standard NBT/BCIP (Promega, Madison, WI, USA). The
139 intensity of each band on the western blot was determined using ImageJ 1.46 software (NIH, <http://imagej.nih.gov/ij/>).

140

141 2.5. Physicochemical properties of quinoa starch

142

142 2.5.1. Amylose determination

143 Amylose content was determined using two methods: a extensively used colorimetry (Apparent amylose-AAP) and a
144 new more accurate enzyme method (Amylose content -AC). Amylose content (AC) of quinoa samples was determined
145 based on a concavalin A (Con A) precipitation procedure and apparent amylose (AAM) content was determined based
146 on the iodine binding method (Li and Zhu, 2018b). For AC determination the K-Amyl kit (Megazyme International, Ltd.,
147 Wicklow, Ireland) was performed according to the manufacturer's instructions. Briefly, starch was dispersed in
148 dimethyl sulphoxide, and the Con A addition precipitated amylopectin. Finally, amylose was hydrolyzed
149 by amyloglucosidase and α -amylase. The absorbance was measured at $\lambda = 510$ nm.

150 For AAM content determination different amylose and amylopectin standards (Sigma, Merck KGaA, Darmstadt,
151 Germany) were used for calibration. The AAM was determinate following Li *et al.*, (2016) procedure. The absorbance
152 was measure at 600 nm using a JASCO V-630 UV-Visible spectrophotometer (JASCO International Co. Ltd. Tokyo).

153

154 2.5.2. Swelling power

155 Swelling power (SP) was analyzed as described by Li *et al.*, (2016) with some modifications. Briefly, starch sample (W0,
156 0.25 g, db) was weighed into a 15 mL centrifuge tube and resuspended in 8 mL deionized water. The tubes were heated
157 over a temperature intervals range of 65–95 °C for 15 min with frequent shaking. Next, the samples were cooled and
158 centrifuged at 2000 x g 20 min. The remained sediment in the centrifuge tube (Ws) were then weighted.

159 The SP of the starch samples was calculated using Eq.

160
$$SP \left(\frac{g}{g} \right) = \frac{W_s}{W_0}$$

161

162 2.5.3. Water-binding capacity (WBC)

163 A suspension of 2.5 g starch (Md) in 37 ml distilled water was agitated for 1 h and centrifuged (3000 x g) for 10 min. The
164 free water was removed from the wet starch. After draining for 10 min, the wet starch was weighed (Mw).

165 The WBC of the sample was calculated as follows:

$$WBC (\%) = \frac{(M_w - M_d)}{M_d} \times 100$$

166 2.6. Thermal properties

167 Thermal analysis was performed using a Differential Scanning Calorimeter (Mettler-Toledo, model 822, Mettler Toledo
168 AG, Greifensee, Switzerland) with a STARe Thermal Analysis System version 8 software (Mettler Toledo AG, Ohio,
169 USA).

170 The instrument calibration was performed using standard compounds (zinc and indium) of defined temperature and heat
171 of fusion. Starch samples (10 mg) were accurately weighed into aluminum DSC pans. Deionized water was added by
172 micropipette (20mg). The sample pans were sealed and equilibrated at 4 °C for 24 h before analysis. An empty sealed
173 pan was used as the reference. All the experiments were performed under nitrogen atmosphere. The samples were
174 heated at 10 °C min⁻¹ from 20 to 90 °C. The onset (To), peak (Tp), and the endset (Te) temperature were recorded.

175 Starch retrogradation was determined on the same gelatinized samples after storage at 4 °C for 7 days. The retrograded
176 starch samples were re-scanned using the heating profile described for starch gelatinization. Gelatinization specific
177 enthalpy of native starch (ΔH_G , J/g) and enthalpy change on reheating of retrograded starch gels (ΔH_R) were calculated
178 by measuring the curve area of the corresponding thermograms. All measurements were performed in triplicate. Degree
179 of retrogradation (%DR) i.e the percentage ratio between the enthalpy change of retrogradation and gelatinization was
180 calculated according to the formula:

$$\%DR = \Delta HR / \Delta HG \times 100$$

181 2.7. Powdered X-ray diffractometry

182 Powder X-ray analysis of the starch samples was performed on a Phillips PW 1730/10 using Cu-K α (1.54 Å) radiation.
183 The accelerating voltage and current were set to 40 kV and 40 mA, respectively, in combination with a scan rate of 1/sec
184 and a step interval of 0.02. The scanning regions of the diffraction angle 2 θ were from 4° to 75°, covering all the
185 significant diffraction peaks of starch samples. After recording the diffractograms, the degree of crystallinity was

186 calculated according to the method described by Nara and Komiyama, (1985). First a smoothed curve was computed
187 connecting the baseline of the peaks in the diffractogram. Then, the area above the smoothed curve and the total area
188 were computed. The degree of crystallinity was calculated as a percentage as follows:

$$\text{Degree of crystallinity} = \frac{A_c}{A_T} \times 100$$

189 Where A_c is the area of the crystalline fraction and A_T is the total area (Roa, Santagapita, Buera, & Tolaba, 2014). The
190 smoothing baseline and the two areas under the curves were calculated using GNU Octave for windows ver. 4.4.1.
191

192

193 **2.8. Scanning electron microscopy**

194 Quinoa starch morphology was examined using a scanning electron microscope SEM Carl Zeiss NTS SUPRA 40
195 (Germany). The samples were sputtered with gold, and then observed and photographed. The micrographs were
196 recorded at 50,000× magnification.

197

198 **2.9. Attenuated Total Reflectance Fourier Transform Infrared Spectra (ATR/FTIR)**

199 Starch extracted from six different quinoa grains were scanned in a Fourier Transform Infrared spectrometer (FT-IR
200 Spectrum 400, Perkin Elmer Inc., Shelton, CT, USA) using an Attenuated Total Reflectance (ATR) accessory. A few
201 milligrams of each powdered sample were placed on a diamond/ZnSe crystal with one reflectance (PIKE Technologies
202 Inc, Madison, WI, USA) and pressed until desired pressure was reached. Spectra were scanned from 600 to 4000 cm^{-1}
203 with a resolution of 4 cm^{-1} until 64 scans were collected at 25 °C. Each sample was scanned in triplicate and the
204 obtained spectra were base line corrected and normalized using Spectrum Software (Perkin Elmer, Inc.). As the ATR
205 crystal showed absorbance peaks from 1800 to 2500 cm^{-1} , this region of the spectra was not considered for further
206 analysis.

207

208 **2.10. Pasting properties of quinoa starch**

209 A rheometer (Paar Physica MCR 300, Anton Paar GmbH, Austria) equipped with a 4.0 cm diameter (CP40) cone and
210 plate geometry was used. Temperature was controlled by a Peltier system (± 0.1 °C). A gap size of 0.5 mm was set, and
211 data points were recorded at a shear rate of 160 rpm. Before measurement, each starch suspension (10 % (w/w)) was
212 stirred manually to disperse the sample homogeneously. The pasting profile of the sample were monitored during

213 thermal treatment according to the method of Chantaro and Pongsawatmanit, (2010), using temperature (T), peak
214 temperature (PKT), peak viscosity (PV), hot paste viscosity (HPV), cool paste viscosity (CPV), as well as, the derivative
215 parameters breakdown ($BD = PV - HPV$), setback ($SB = CPV - HPV$), stability ratio ($SR = 100 \times HPV/PV$), and setback
216 ratio ($BR = CPV/HPV$) were calculated for each genotype according Li *et al.*, (1997).

217

218 **2.11. Statistical analysis**

219 All determinations were performed at least in triplicate. The data were expressed as the mean values \pm SD. Statistical
220 tests were applied using GraphPad Prism version 6.00 for Windows, GraphPad Software, La Jolla California USA,
221 www.graphpad.com). When applicable, data were analyzed by one-way Analysis of variance (ANOVA), and differences
222 between genotypes were determined following Tukey HSD post-hoc test, at $P \leq 0.05$. The relationships between different
223 properties of starches were also determined using Pearson correlation coefficients. Statistical significance was defined
224 as $P < 0.05$. Principal component analysis (PCA) was performed after normalization (using min-max algorithm) of the
225 variables from pasting properties for each starch sample using Infostat/ p2011 software, Universidad de Córdoba,
226 Córdoba, Argentina.

227 **3. RESULTS AND DISCUSSION**

228 **3.1. Physicochemical properties**

229 **3.1.1. Amylose content**

230 Considering differences in amylose content, cereals can be classified in three different categories, i) normal amylose
231 (28%) corn, wheat starches, ii) high amylose (50-70%) corn starch and iii) low amylose (<2%) for waxy maize starch
232 (Fennema's Food Chemistry, 2008). Despite quinoa genotypes did not shown such a variability, slight statistical
233 differences in their amylose content were found as reported by other authors (Jan et al 2017; Li et al 2016, 2018;
234 Lindeboom et al. 2005, Steffolani et al 2013.) The AC differences ranged from 7.2 % (CHEN 426) to 10.1 % (INTA-
235 Hornillos), and the AAM from 9.8 % (CHEN 252) to 12.3 % (CHEN 420) (Table 1). Similarly, AC values between 6.06 to
236 8.44 and an AAM range of 7.50 to 10.88 were reported for other quinoa genotypes (Li & Zhu, 2018a). The differences
237 between methods may explain the AAM tendency to overestimate amylose content due to the formation of amylopectin-
238 iodine complexes (Gibson et al., 1997). Also, the AAM relatively large standard deviation could be attributed to the
239 quinoa grain low amylose content (Martinez, 1996)(Martinez et al., 1996). Many parameters, such as genetics, maturity,
240 and growing conditions, may influence the grain amylose content (G. Li et al., 2016).

241 **3.1.2. Swelling power (SP) and water-binding capacity (WBC)**

242

243 The SP and WBC of quinoa starch genotypes are shown in Table 1. Significant differences in the quinoa genotypes SP
244 were observed. As temperature raised the quinoa genotypes SP increased, disrupting the granule structure by
245 weakening their internal associative forces in all quinoa genotypes starches. Since amylopectin/amylose ratio influences
246 SP some authors looked for an amylose content-SP correlation having found it negative (Sasaki, Yasui, & Matsuki,
247 2000). Similarly, in the present work a negative correlation between the SP and the AC was observed at 65°C, 75°C and
248 85°C ($r = -0.856, -0.929, -0.904$, respectively $P < 0.05$). Other authors, have found that various parameters also influence
249 starches SP: average granule size, gelatinization peak temperature (J.-Y. Li & Yeh, 2001), starch chains interaction,
250 amylose and amylopectin molecular weight/distribution, degree and length of branching and conformation (Singh et al.,
251 2003) (G. Li & Zhu, 2018a). Further studies on the quantity of short internal chains of the different genotypes here
252 evaluated are necessary to elucidate the quinoa starch granule structure.

253

254 3.2. Thermal properties of Native and Retrograded starches

255 The DSC curves of starch gelatinization of the six genotypes studied are presented in Fig.1A. Thermal transition
256 temperatures of native starches and retrograded starches determined by DSC are summarized in Table 2. The onset
257 gelatinization temperature (T_o), the peak temperature (T_p) and the endset temperature (T_e) values obtained range from
258 58.0 to 67.9, 62.2 to 75.1 and 74.6 to 85.8 °C, respectively. The transition temperature ranged ($T_e - T_o$) from 15.2 to 22.1
259 °C. The highland genotype CHEN 420 and dry valley genotype INTA-Hornillos, had higher onset and endset
260 temperatures. The gelatinization enthalpy (ΔH_G) ranged from 9.8 to 12.2 J/g. The T_o , T_p , T_e , ($T_e - T_o$) and ΔH_G differed
261 significantly ($P < 0.05$) between genotypes. This is probably due to different quantities of longer chains in amylopectin
262 (G. Li et al., 2016; Singh et al., 2003). The onset temperature correlated positively with the amylose content ($r = 0.90$). No
263 significant correlations were found between the amylose content and T_p or T_e . Starch retrogradation was observed
264 when the gelatinized samples were stored at 4 °C for 7 days (Table 2). The enthalpy of retrogradation (ΔH_R) and
265 retrogradation percentage (% DR) for starches isolated from the different genotypes ranged from 1.9 to 3.5 J/g; and from
266 17.7 to 32 % up to 7 days storage, respectively. The quinoa starch retrogradation degree was positively correlated to
267 amylose content. The ΔH_R and %DR increased as the gels become less soluble due to starch molecules
268 recrystallization. According to Steffolani et al., (2013) quinoa starches exhibited lower %DR when compared to other
269 pseudocereals. A thorough understanding of starch gelatinization and retrogradation is needed to control starch
270 functional properties for food processing, human nutrition and industrial applications.

3.3. Crystalline properties of quinoa starches

271
272 The XRD diffractograms of these starches give the stronger diffraction peaks at around 15, 17, 18 and 23° (2 θ), all
273 exhibited a typical A type, indicating that they share similar crystalline patterns (Fig1). Crystallinity is affected by amylose
274 content and proportions of different chain length in amylopectin (Cheetham & Tao, 1998). The relative crystallinity,
275 calculated from the XRD patterns, were almost identical: 28.5, 28.4, 27.6, 27.5, 26.6 and 26.1 % for CHEN 426, 182,
276 252,435 420, INTA- Hornillos, respectively, these values were inversely proportional to the amylose content. Crystallinity
277 values between 21.5 and 43 % have been previously reported for starch isolated from quinoa (G. Li & Zhu, 2018a).

3.4. ATR/FTIR spectra collected from the starch fractions of each quinoa genotypes

278
279 Fig.1 C shows the normalized ATR/FTIR spectra for CHEN 182 and CHEN 420 genotypes. Spectra show a broad
280 absorption band from 3010 to 3750 cm⁻¹ associated mainly with hydroxyl groups present in carbohydrates, due to OH
281 stretching. Moreover, a small band with at least two overlapped peaks is observed from 2800 to 3000 cm⁻¹, this band is
282 associated mainly to C-H stretching. Besides, a small broad band from 1200 to 1500 cm⁻¹ is represented by CH₂OH side
283 chain related mode, C-O-H bending, CH₂ twisting, CH₂ bending and C-O-O stretching. Finally, spectra show a strong
284 absorption band, from 900 to 1200 cm⁻¹ associated to C-O and C-C stretching (1163 cm⁻¹), C-O-H bending (1094 cm⁻¹)
285 and C-H bending (1067 cm⁻¹). Additionally, below 900 cm⁻¹, small bands can be observed due to skeletal modes of the
286 pyranose ring (Warren, Gidley, & Flanagan, 2016). The spectra analyzed in Fig. 1 C shows no significant differences
287 between the starches from the dry valley (CHEN 182) and the highland (CHEN 420) genotypes. The same pattern was
288 observed for all the genotypes analyzed i.e. CHEN 252, CHEN 426, CHEN 435 and INTA-Hornillos (Spectra non-
289 shown).

3.5. Scanning electron microscope of quinoa starch granule

290
291 The starch granule morphology of the six genotypes was examined using SEM. The granules showed polygonal and
292 irregular shapes (Fig. 2 A) The granule size ranging from 0.5 to 1.8 μ m is smaller than cereal starches, providing
293 exclusive properties for pharmaceutical and cosmetic industry. Starch granule structure suitability for a food
294 manufacturing process or its nutritional qualities depends on i) the grain genetic ii) the environmental factors that control
295 starch biosynthesis iii) and how the material is processed. For example, small starch granules were associated with high
296 rupture resistance and high stability against shearing (Jan et al., 2017; Steffolani et al., 2013). Moreover, small sized
297 starch is required for specific applications in food industry such as fat replacer (Lindeboom, Chang, & Tyler, 2004), flavor

298 encapsulation by spray drying – and as a thickener agent in cosmetic industry (Lindeboom et al., 2004, Feng, Wang,
299 Chen, Pan, & Tu, 2018).

300 3.6. Quinoa Starch granule-bound proteins

301 Amylose is mainly produced via the activity of granule-bound starch synthase. The accumulation of the amylose fraction
302 of starch is controlled by a single dominant gene in quinoa, *GBSS* (Brown, Cepeda-Cornejo, Maughan, & Jellen, 2015).

303 To characterize the accumulation of GBSS from different quinoa genotypes, protein extracts were separated by SDS-
304 PAGE, as mentioned in methods (Fig 2 B upper panel). The electrophoresis showed the presence of two bands of a
305 molecular weight of approximately ~63 and ~56 kDa for quinoa genotypes and one band of ~57 kDa for rice both
306 polypeptides reacted with rice GBSSI (Fig 2 B lower panel). The proteins were transferred into a nitrocellulose
307 membrane and antibodies specific to rice GBSSI were used. The western blot showed that both the ~63- and the ~56
308 kDa quinoa polypeptides reacted with rice GBSSI (Fig 2 B lower panel). The accumulation of CHEN182 and CHEN 426
309 GBSS, both genotypes with lower amylose content, was ~1/4 times lower than INTA- Hornillos mature GBSS (Fig 2 B
310 lower panel).

311 Lindeboom et al. (2005) identified two quinoa GBSSI proteins with molecular masses of 62- and 56 kDa and showed that
312 quinoa lines with high amylose (19.5%) had larger bands than that of intermediate amylose content (13.5%) by
313 immunoblot analysis. These authors also suggested these two proteins that immunoreacted with wheat GBSS were
314 different isoforms. According to Brown et al. (2015) the two bands identified correspond to the full-length and mature
315 GBSS proteins. The protein is localized within the central core of the starch grains and the mature *Chenopodium* GBSS
316 consensus protein sequence was conserved across wheat, maize and rice (Brown et al., 2015). Investigation on the
317 genetic variability of quinoa genotypes possessing higher and lower amylose content could be useful for novel
318 technological and nutritional value of starch. For example, the reduction in amylose content via GBSS modification in
319 cassava starch enhanced clarity and stability properties making it useful for paper and textile industries, also as making
320 food products such dairy and noodles (Tappiban, Smith, Triwitayakorn, & Bao, 2019). For potato lines, suppression of
321 GBSS demonstrates a combined rheological, crystalline and degradability functionalities (Wang & Copeland, 2015 and
322 references therein).

323 3.7. Pasting properties

324 Significant differences in the pasting characteristics were observed between the starches of the quinoa genotypes
325 studied (Table 3, Fig. 3A). Pasting temperature (PT) is the temperature at which starch molecules hydrate and the
326 suspension viscosity increases abruptly. The PT values obtained, which ranged from 62 (CHEN 252) to 65.1 °C (CHEN
327 426), were similar to the DSC T_0 values obtained as well as to other quinoa starch values previously reported (Jan et al.,
328 2017; G. Li et al., 2016). PT and peak temperature (PKT) are highly dependent on the swelling granule behavior and
329 WBC (Jan et al., 2017; Kong et al., 2015; G. Li et al., 2016). Both parameters are also associated with granule rigidity
330 and with different degree of branching and crystallinity (Jan et al., 2017; Kim & Wiesenborn, 1996; Wang, Li, Copeland,
331 Niu, & Wang, 2015 and references therein).

332 Peak viscosity (PV), which is related to starch swelling power (Kong et al., 2015), showed the maximum viscosity
333 attained by quinoa starch samples while heating. In addition to PV, Hot Viscosity (HV-at 95°C) and Cool Viscosity (CV-at
334 50°C) are key factors for quinoa starch industrial processing, transport and applications. The INTA-Hornillos genotype
335 showed the highest viscosity parameters (PV, HV, and CV), which can be related to its high AC, WBC, and SP values at
336 95°C. On the other hand, the highland genotypes CHEN 420 and CHEN 426 showed lower PV and stable viscosity
337 values, evidenced by their low breakdown parameter (BD). Both genotypes had the same pasting curve, a tendency that
338 may be associated with their ecological origin. The highland genotypes are plants with shorter crop cycle (90 to 110 days
339 from sowing to harvest) and greater temperature sensitivity influencing the rate of flowering, than the dry valley
340 genotypes (130 to 140 days from sowing to harvest). The dry valley genotypes showed similar pasting curves, except
341 INTA-Hornillos, which is from the inter-Andean Valley of Peru and has been cultivated in northwestern Argentina for
342 more than 30 years. Thus, the effect of the genotypic background and environment became evident on the pasting
343 curves. The composition of different starches is susceptible to environmental variation, especially growth temperature
344 (Tester & Karkalas, 2001). The evaluation of these parameters may be a useful tool to discriminate between ecological
345 area and quinoa genotypes and the differences among these genotypes and their desirable properties.

346 It is worth noticing that multiple factors, such as particle size distribution, internal and external chain length, and granule
347 strength, influence the rheological analysis of quinoa starch (G. Li & Zhu, 2018b). Quinoa starch is a complex system
348 and the pasting process implies different variables such as molecular diffusion, granule rigidity and degree of damage,
349 amylose content, solubility, and degree of crystallinity (Jan et al., 2017). The analysis of differences in pasting
350 parameters may allow identifying a quinoa genotype that provides desirable properties for a specific technological use,

351 as reported by (Kim & Wessendorf, 1990) in a particular potato genotype whose starch had high setback ratio, providing
352 excellent attributes for noodle preparation.

353 3.8. Principal component analysis (PCA)

354 PCA was performed to further explore the relationship between the pasting properties and the ecological origin of the
355 genotypes. Figure 3B shows the biplot (scores and loadings) using the pasting properties (nine normalized variables) as
356 the input variables for PCA. The two first principal components (PC1 and PC2) accounted for a total accumulated
357 variance of about 94% of the original data set and clearly discriminate the quinoa samples into three well-defined groups:
358 one composed of quinoa grains from the highlands (CHEN 420 and 426), another one composed of three of the four
359 genotypes from the dry valley (CHEN 182, 252 and 435), and the last one composed of the INTA-Hornillos genotype.
360 The possible reason of the third group arrangement could be the ancestor of this last genotype, which originated from a
361 quinoa *var. CICA* grown in the dry valleys of Peru. According to the PCA results recorded with the nine variables used in
362 this work, similar quinoa grains showed a similar pasting profile. The arrows in the biplot represent the relative weight of
363 each variable to each component. The most relevant variables influencing to PC1 are PV, BD and SR, and for the PC2
364 are PT and PKT. Lastly, CV, HC and SB show low relevance and are highly correlated.

365 4. CONCLUSIONS

366 Screening the natural variability present in germplasm banks allows for the identification of interesting and unusual
367 genotypes properties. The characterization of the physicochemical and functional starch properties provides tools to
368 identify genotypes with industrial and commercial potential.

370 The physicochemical, thermal, and pasting properties of the starch of six quinoa genotypes native to the highlands and
371 dry valleys of northwestern Argentina were here studied. Significant differences were observed among the six quinoa
372 genotypes studied in AC, SP, WBC, thermal and pasting properties. The pasting properties led to a good clustering of
373 the genotypes according to their ecological origin and genotype background. This finding suggests that the higher PKT
374 values and lower PV and BD values of the highland genotypes might be related to higher environmental temperatures
375 during grain filling.

376 To the best of our knowledge, this is the first report of the characterization of quinoa starch properties related to their
377 ecological origin and genotype background. The current research is part of our broader goal of completing the
378 characterization of a wider set of quinoa starches from different germplasm and environments, with the final objective of

379 attaining useful information regarding desirable new industrial applications. Likewise, promoting the development of
380 cultivation in historically neglected regions by expanding the agricultural frontier.

381

382 **ACKNOWLEDGEMENTS**

383 This work was supported by Agencia Nacional de Promoción Científica y Tecnológica, ANPCyT, (PICT 2013-1331 to
384 MPB 2016-2851 to MPLF), CONICET (PIP 11220170100042CO) and Universidad de Buenos Aires (UBACYT
385 20020130100443BA). We thank Ing. Castro for providing us the material used in this study and Dr. Agüero (Instituto
386 Nacional de Tecnología Agropecuaria-(INTA) for helpful suggestions.

387 **REFERENCES**

388

389 Bahaji, A., Li, J., Sánchez-López, Á. M., Baroja-Fernández, E., Muñoz, F. J., Ovecka, M., ... Pozueta-Romero, J. (2014).

390 Starch biosynthesis, its regulation and biotechnological approaches to improve crop yields. *Biotechnology*
391 *Advances*, 32(1), 87–106. <https://doi.org/10.1016/j.biotechadv.2013.06.006>

392 Brown, D. C., Cepeda-Cornejo, V., Maughan, P. J., & Jellen, E. N. (2015). Characterization of the Granule-Bound Starch
393 Synthase I Gene in Chenopodium. *The Plant Genome*, 8(1), 0. <https://doi.org/10.3835/plantgenome2014.09.0051>

394 Burrieza, H. P., López-Fernández, M. P., & Maldonado, S. (2014). Analogous reserve distribution and tissue
395 characteristics in quinoa and grass seeds suggest convergent evolution. *Frontiers in Plant Science*, 5(October),
396 546. <https://doi.org/10.3389/fpls.2014.00546>

397 Chantaro, P., & Pongsawatmanit, R. (2010). Influence of sucrose on thermal and pasting properties of tapioca starch
398 and xanthan gum mixtures. *Journal of Food Engineering*, 98(1), 44–50.
399 <https://doi.org/10.1016/j.jfoodeng.2009.12.006>

400 Cheetham, N. W. ., & Tao, L. (1998). Variation in crystalline type with amylose content in maize starch granules: an X-
401 ray powder diffraction study. *Carbohydrate Polymers*, 36(4), 277–284. [https://doi.org/10.1016/S0144-8617\(98\)00007-1](https://doi.org/10.1016/S0144-8617(98)00007-1)

403 Curti, R. N., de la Vega, A. J., Andrade, A. J., Bramardi, S. J., & Bertero, H. D. (2014). Multi-environmental evaluation for
404 grain yield and its physiological determinants of quinoa genotypes across Northwest Argentina. *Field Crops*

- 405
406 Fujita, N., Yoshida, M., Asakura, N., Ohdan, T., Miyao, A., Hirochika, H., & Nakamura, Y. (2006). Function and
407 Characterization of Starch Synthase I Using Mutants in Rice. *Plant Physiology*, *140*(3), 1070–1084.
408 <https://doi.org/10.1104/pp.105.071845>
- 409 Gibson, T. S., Solah, V. a., & McCleary, B. V. (1997). A Procedure to Measure Amylose in Cereal Starches and Flours
410 with Concanavalin A. *Journal of Cereal Science*, *25*(2), 111–119. <https://doi.org/10.1006/jcres.1996.0086>
- 411 Jan, K. N., Panesar, P. S., Rana, J. C., & Singh, S. (2017). Structural, thermal and rheological properties of starches
412 isolated from Indian quinoa varieties. *International Journal of Biological Macromolecules*, *102*, 315–322.
413 <https://doi.org/10.1016/j.ijbiomac.2017.04.027>
- 414 Kim, Y. S., & Wiesenborn, D. P. (1996). Starch noodle quality as related to potato genotypes. *Journal of Food Science*,
415 *61*(1), 248–252. <https://doi.org/10.1111/j.1365-2621.1996.tb14771.x>
- 416 Kong, X., Zhu, P., Sui, Z., & Bao, J. (2015). Physicochemical properties of starches from diverse rice cultivars varying in
417 apparent amylose content and gelatinisation temperature combinations. *Food Chemistry*, *172*, 433–440.
418 <https://doi.org/10.1016/j.foodchem.2014.09.085>
- 419 Li, G., Wang, S., & Zhu, F. (2016). Physicochemical properties of quinoa starch. *Carbohydrate Polymers*, *137*, 328–338.
420 <https://doi.org/10.1016/j.carbpol.2015.10.064>
- 421 Li, G., & Zhu, F. (2018a). Quinoa starch: Structure, properties, and applications. *Carbohydrate Polymers*, *181*(November
422 2017), 851–861. <https://doi.org/10.1016/j.carbpol.2017.11.067>
- 423 Li, G., & Zhu, F. (2018b). Rheological properties in relation to molecular structure of quinoa starch. *International Journal*
424 *of Biological Macromolecules*, *114*, 767–775. <https://doi.org/10.1016/j.ijbiomac.2018.03.039>
- 425 Li, J.-Y., & Yeh, A.-I. (2001). Relationships between thermal, rheological characteristics and swelling power for various
426 starches. *Journal of Food Engineering*, *50*(3), 141–148. [https://doi.org/10.1016/S0260-8774\(00\)00236-3](https://doi.org/10.1016/S0260-8774(00)00236-3)
- 427 Li, W., Lin, R., & Corke, H. (1997). Physicochemical Properties of Common and Tartary Buckwheat Starch. *Cereal*
428 *Chemistry Journal*, *74*(1), 79–82. <https://doi.org/10.1094/CCHEM.1997.74.1.79>
- 429 Lindeboom, N., Chang, P. R., Falk, K. C., & Tyler, R. T. (2005). Characteristics of Starch from Eight Quinoa Lines.

- 430 *Cereal Chemistry Journal*, 82(2), 210–222. <https://doi.org/10.1094/CC-02-0210>
- 431 Lindeboom, N., Chang, P. R., & Tyler, R. T. (2004). Analytical, Biochemical and Physicochemical Aspects of Starch
432 Granule Size, with Emphasis on Small Granule Starches: A Review. *Starch - Stärke*, 56(34), 89–99.
433 <https://doi.org/10.1002/star.200300218>
- 434 Lindeboom, N., Chang, P. R., Tyler, R. T., & Chibbar, R. N. (2005). Granule-Bound Starch Synthase I (GBSSI) in Quinoa
435 (*Chenopodium quinoa* Willd.) and Its Relationship to Amylose Content. *Cereal Chemistry Journal*, 82(3), 246–250.
436 <https://doi.org/10.1094/CC-82-0246>
- 437 López-Fernández, M. P., & Maldonado, S. (2013). Programmed cell death during quinoa perisperm development.
438 *Journal of Experimental Botany*, 64(11), 3313–3325. <https://doi.org/10.1093/jxb/ert170>
- 439 Martínez, C. (1996). Determination of amylose in flour by a colorimetric assay: Collaborative study. *Starch/Stärke*,
440 48(3), 86–89. <https://doi.org/10.1002/star.19960480303>
- 441 Nara, S., & Komiya, T. (1983). Studies on the Relationship Between Water-saturated State and Crystallinity by the
442 Diffraction Method for Moistened Potato Starch. *Starch - Stärke*, 35(12), 407–410.
443 <https://doi.org/10.1002/star.19830351202>
- 444 Peng, J., Wang, Y., Chen, G., Pan, L., & Tu, K. (2018). Morphological and Physicochemical Properties of Very Small
445 Granules Starch from *Agriophyllum squarrosum* (L.) Moq. in Comparison with Maize Starch. *Starch - Stärke*, 70(3–
446 4), 1700068. <https://doi.org/10.1002/star.201700068>
- 447 Roa, D. F., Santagapita, P. R., Buera, M. P., & Tolaba, M. P. (2014). Amaranth Milling Strategies and Fraction
448 Characterization by FT-IR. *Food and Bioprocess Technology*, 7(3), 711–718. <https://doi.org/10.1007/s11947-013-1050-7>
- 449 1050-7
- 450 Sasaki, T., Yasui, T., & Matsuki, J. (2000). Effect of amylose content on gelatinization, retrogradation, and pasting
451 properties of starches from waxy and nonwaxy wheat and their F1 seeds. *Cereal Chemistry*, 77(1), 58–63.
452 <https://doi.org/10.1094/CCHEM.2000.77.1.58>
- 453 Singh, N., Singh, J., Kaur, L., Singh Sodhi, N., & Singh Gill, B. (2003). Morphological, thermal and rheological properties
454 of starches from different botanical sources. *Food Chemistry*, 81(2), 219–231. [https://doi.org/10.1016/S0308-
455 8146\(02\)00416-8](https://doi.org/10.1016/S0308-8146(02)00416-8)

- 456 Smith, A. M. (2001). The biosynthesis of starch granules. *Biomacromolecules*, 2(2), 333–341.
457 <https://doi.org/10.1021/bm000133c>
- 458 Steffolani, M. E., León, A. E., & Pérez, G. T. (2013). Study of the physicochemical and functional characterization of
459 quinoa and kañiwa starches. *Starch/Staerke*, 65(11–12), 976–983. <https://doi.org/10.1002/star.201200286>
- 460 Tappiban, P., Smith, D. R., Triwitayakorn, K., & Bao, J. (2019). Recent understanding of starch biosynthesis in cassava
461 for quality improvement: A review. *Trends in Food Science and Technology*, 83(July 2018), 167–180.
462 <https://doi.org/10.1016/j.tifs.2018.11.019>
- 463 Tester, R. F., & Karkalas, J. (2001). The effects of environmental conditions on the structural features and physico-
464 chemical properties of starches. *Starch/Staerke*, 53(10), 513–519. [https://doi.org/10.1002/1521-379X\(200110\)53:10<513::AID-STAR513>3.0.CO;2-5](https://doi.org/10.1002/1521-379X(200110)53:10<513::AID-STAR513>3.0.CO;2-5)
- 465
- 466 Wang, S., & Copeland, L. (2015). Effect of Acid Hydrolysis on Starch Structure and Functionality: A Review. *Critical*
467 *Reviews in Food Science and Nutrition*, 55(8), 1081–1097. <https://doi.org/10.1080/10408398.2012.684551>
- 468 Wani, A. A., Singh, P., Shah, M. A., Schweiggert-Weisz, U., Gul, K., & Wani, I. A. (2012). Rice Starch Diversity: Effects
469 on Structural, Morphological, Thermal, and Physicochemical Properties-A Review. *Comprehensive Reviews in*
470 *Food Science and Food Safety*, 11(5), 417–436. <https://doi.org/10.1111/j.1541-4337.2012.00193.x>
- 471 Warren, F. J., Gidley, M. J., & Flanagan, B. M. (2016). Infrared spectroscopy as a tool to characterise starch ordered
472 structure—a joint FTIR–ATR, NMR, XRD and DSC study. *Carbohydrate Polymers*, 139, 35–42.
473 <https://doi.org/10.1016/j.carbpol.2015.11.066>
- 474 Zi, Y., Ding, J., Song, J., Humphreys, G., Peng, Y., Li, C., ... Guo, W. (2018). Grain Yield, Starch Content and Activities
475 of Key Enzymes of Waxy and Non-waxy Wheat (*Triticum aestivum* L.). *Scientific Reports*, 8(1), 250100.
476 <https://doi.org/10.1038/s41598-018-22587-0>

477

478 **Table 1. Amylose content, swelling power and water binding capacity of the starches of the quinoa genotypes**
479 **studied**

480 *a* (Curti et al., 2014), *b* provided by the National Institute of Agricultural Technology (INTA- Abra Pampa, Argentina)
481 (INTA Abra Pampa – Argentina. Values are means \pm SD. Values in the same column followed by the same letter are not
482 significantly different ($P < 0.05$, $n=3$)

483 **Table 2. Thermal transition temperatures of the six quinoa starch samples.**

484 Values are means \pm SD. Values in the same column followed by the same letter are not significantly different ($P < 0.05$,
485 $n=3$). *To*, onset temperature; *T_p*, peak temperature; ΔH , gelatinization enthalpy; *T_e*, conclusion temperature; *T_e-T_o*,

486 **Table 3. Pasting properties of the starches of the quinoa genotypes studied.**

487 Values in the same column followed by the same letter are not significantly different ($P < 0.05$) ($n=3$). *PT* pasting
488 temperature; *PKT* peak temperature; *PV* peak viscosity; *HV* hot viscosity; *CV* cool viscosity; *BD* breakdown (*PV-HV*); *SB*
489 setback (*CV-HV*); *SR* stability ratio ($100 \cdot HV/PV$); *BR* setback ratio (*CV/HV*).

490

491

492

493

494

495

496

497

498

499

500

501

502

503

504

505

506

507

508

509

510

511

512

513 Table 1. Amylose content, swelling power and water binding capacity of the starches of the quinoa genotypes

Genotypes	Genotypes group ecoregion	Genotype origin	AC (%)	AAM (%)	Swelling Power at				Water Binding (%)
					65 °C	75 °C	85 °C	95 °C	
CHEN 182 ^a	Dry valleys	QQ 95-NSL 106394, Humahuaca (Jujuy)	7.7 ± 0.2 ^{bc}	10.5 ± 0.5 ^a	6.5 ± 0.3 ^{ab}	9.0 ± 0.2 ^a	11.3 ± 0.3 ^a	10.7 ± 0.1 ^c	90.4 ± 0.4 ^a
CHEN 252 ^a	Dry valleys	Maimará, Tilcara (Jujuy)	8.3 ± 0.2 ^{bc}	9.8 ± 0.6 ^a	7.0 ± 0.1 ^a	8.5 ± 0.5 ^{ab}	10.9 ± 0.1 ^a	11.8 ± 0.2 ^b	81.3 ± 0.1 ^c
CHEN 435 ^a	Dry valleys	Cangrejillos, Yavi (Jujuy)	8.9 ± 0.0 ^{ab}	11.1 ± 0.1 ^a	5.8 ± 0.1 ^{bc}	8.5 ± 0.1 ^{ac}	10.7 ± 0.1 ^a	9.0 ± 0.1 ^d	85.1 ± 0.1 ^b
CHEN 420 ^a	Highlands - Puna	Antofallita, Los Andes (Salta)	9.4 ± 0.0 ^a	12.3 ± 0.5 ^a	6.0 ± 0.2 ^{abc}	7.6 ± 0.2 ^{bc}	8.8 ± 0.2 ^b	11.1 ± 0.1 ^c	81.0 ± 0.3 ^c
CHEN 426 ^a	Highlands - Puna	Santa Rosa de los Pastos Grandes, Los Andes (Salta)	7.2 ± 0.0 ^c	10 ± 1 ^a	6.6 ± 0.1 ^{ab}	9.2 ± 0.2 ^a	11.0 ± 0.3 ^a	13.0 ± 0.1 ^a	90.2 ± 0.8 ^a
INTA-Hornillos ^b	Dry valleys	Hornillos (Jujuy)	10.1 ± 0.4 ^a	12 ± 2 ^a	5.3 ± 0.3 ^d	7.6 ± 0.4 ^{bc}	8.6 ± 0.1 ^b	12.4 ± 0.3 ^b	88.3 ± 0.3 ^a
Mean			8.6	11.01	6.2	8.2	10.2	11.3	86.06

514 **studied**

515

516

Table 2. Thermal transition temperatures of the six quinoa starch samples.

Genotypes	Gelatinization					Retrogradation ₅₁₉	
	ΔH_G (J/g)	T_o (°C)	T_p (°C)	T_e (°C)	$T_e - T_o$ (°C)	ΔH_R (J/g)	DR_{520} (%)
CHEN 182	11.7 ± 0.1^{ab}	61.2 ± 0.2^b	74.3 ± 0.3^{bc}	83.3 ± 1.3^a	22.1 ^a	2.4 ± 0.2^{ab}	20.6 ^{ab}
CHEN 252	12.2 ± 0.8^a	65.7 ± 0.4^a	72.0 ± 0.0^b	82.7 ± 0.7^a	17.0 ^{ab}	3.1 ± 0.3^{ab}	25.3 ^{ab}
CHEN 435	9.8 ± 0.5^b	65.7 ± 0.3^a	72.5 ± 0.1^{bc}	80.8 ± 1.6^{ab}	15.2 ^b	2.4 ± 0.2^{ab}	24.3 ^{ab}
CHEN 420	10.1 ± 0.5^{ab}	67.9 ± 0.3^a	74.0 ± 1.1^{bc}	85.8 ± 1.7^a	17.9 ^{ab}	3.2 ± 0.3^{ab}	31.6 ^a
CHEN 426	10.4 ± 0.2^{ab}	58.0 ± 0.2^c	64.2 ± 0.1^d	74.6 ± 0.5^b	16.6 ^{ab}	1.9 ± 0.2^b	17.7 ^b
INTA-Hornillos	10.9 ± 0.3^{ab}	67.3 ± 1.5^{ba}	75.1 ± 0.0^a	83.6 ± 1.2^a	16.3 ^{ab}	3.5 ± 0.4^a	32 ^a

Journal Pre-proof

521 Table 3. Pasting properties of the starches of the quinoa genotypes studied.

Genotypes	PT (°C)	PKT (°C)	PV (Pa.s)	HV (Pa.s)	CV (Pa.s)	BD (Pa.s)	SB (Pa.s)	SR	BR
CHEN 182	62.8± 0.1 ^b	66.8 ± 0.2 ^b	60 ± 7 ^b	16 ± 2 ^{bc}	28 ± 9 ^b	44 ± 9 ^b	12 ± 7 ^{bc}	26 ± 6 ^d	1.7 ± 0.3 ^a
CHEN 252	62.0± 0.1 ^c	68 ± 1 ^b	41 ± 6 ^c	18 ± 2 ^b	28 ± 7 ^b	23 ± 4 ^c	11 ± 5 ^{bc}	43 ± 2 ^c	1.6 ± 0.2 ^a
CHEN 435	62.5± 0.2 ^b	66 ± 1 ^{bc}	44 ± 7 ^c	17 ± 4 ^b	28 ± 2 ^b	27 ± 3 ^c	11 ± 2 ^b	30 ± 7 ^d	1.7 ± 0.3 ^a
CHEN 420	63± 1 ^b	88 ± 10 ^a	12 ± 3 ^d	7 ± 3 ^d	12 ± 4 ^c	5 ± 2 ^d	5 ± 1 ^c	65 ± 9 ^b	1.7 ± 0.2 ^a
CHEN 426	65.1± 0.3 ^a	92 ± 2 ^a	14 ± 1 ^d	14 ± 1 ^c	27 ± 2 ^b	0 ± 2 ^d	12 ± 3 ^b	102 ± 11 ^a	1.8 ± 0.2 ^a
INTA-Hornillos	62.1± 0.1 ^c	65.7 ± 0.2 ^c	127 ± 1 ^a	52 ± 1 ^a	89 ± 2 ^a	75 ± 1 ^a	36 ± 1 ^a	41 ± 1 ^c	1.7 ± 0.1 ^a

522

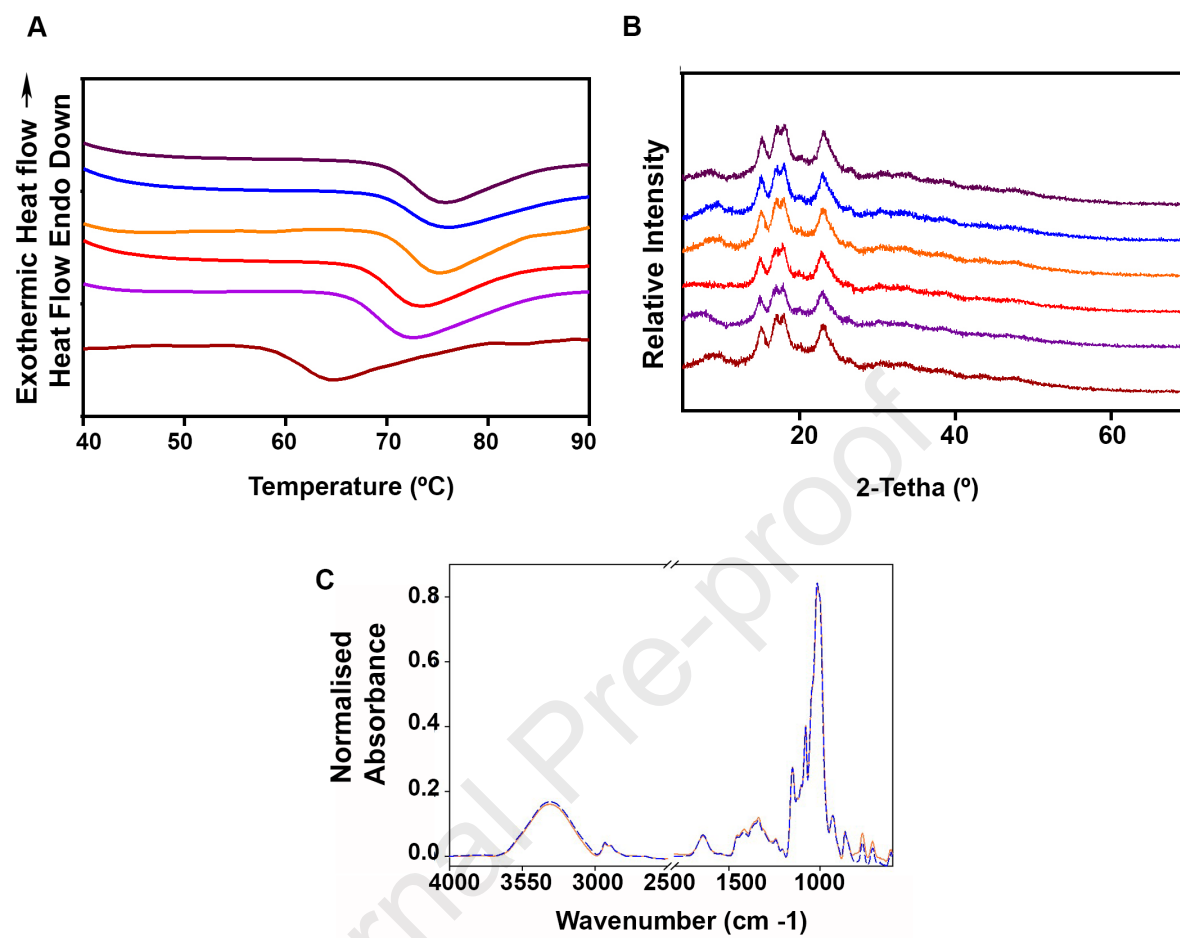
523 **Figure 1. DSC thermograms (A) XRD patterns (B) and FTIR spectra (C) of the quinoa starches studied.** In A and
 524 B, INTA -Hornillos (purple), CHEN 420 (blue), CHEN 182 (orange), CHEN 435 (red), CHEN 252 (light purple), CHEN
 525 426 (brown). In C, CHEN 420 blue dotted line, CHEN 182 continuous line.

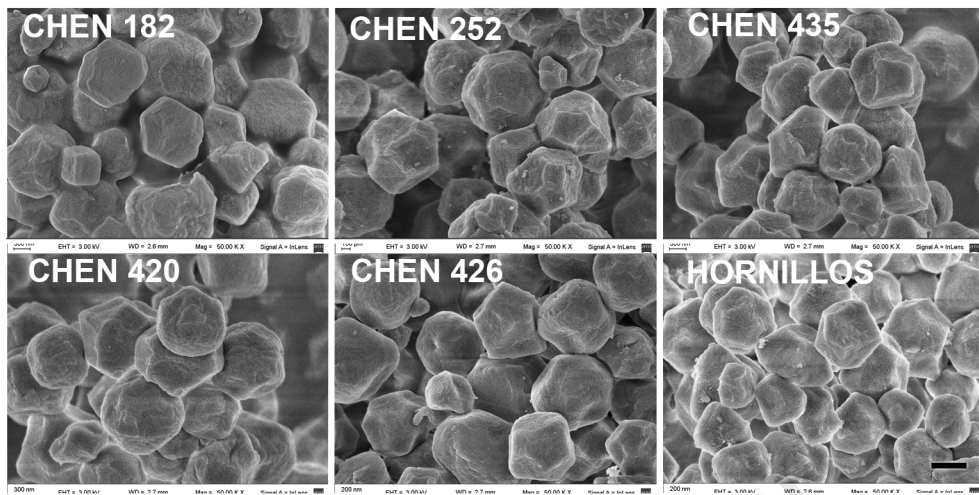
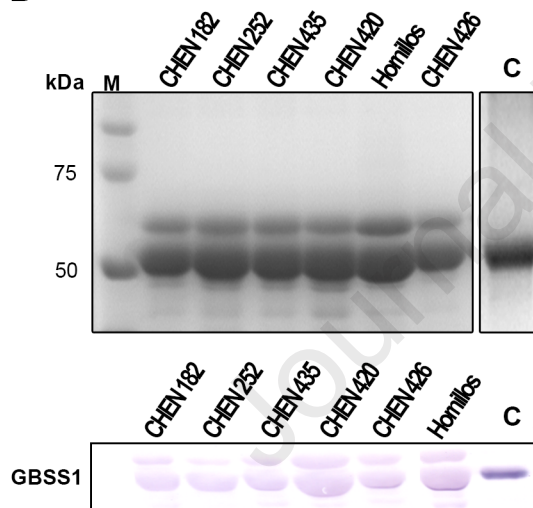
526 **Figure 2. A) Scanning electron microscopy (SEM) micrograph at 50.000× magnification, of the isolated starch**
 527 **granules.** (Scale bar = 600 nm) **B) Quinoa GBSS from the isolated starch was subjected to SDS- PAGE (upper**
 528 **panel) and western blotting, probed with antibody specific for GBSS rice (lower panel).**

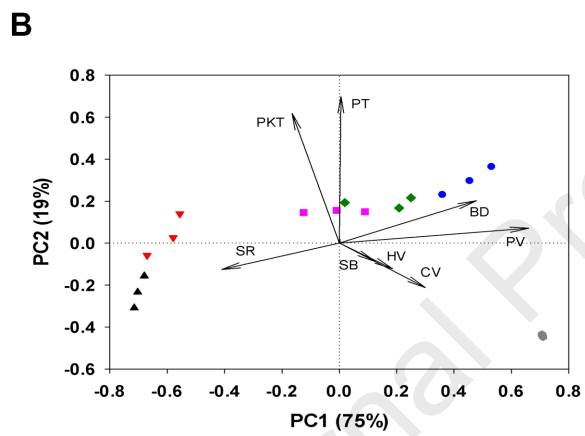
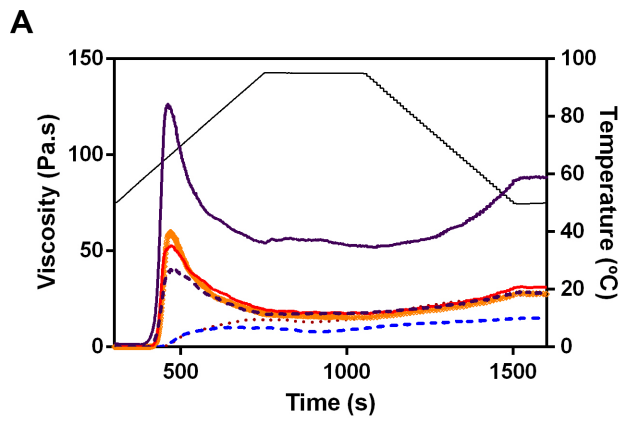
529 **Figure 3. A) Pasting properties of the starches of the quinoa genotypes studied.** CHEN 182 (orange solid line),
 530 CHEN 252 (purple dotted line), CHEN 435 (red solid line), CHEN 420 (blue dash line), CHEN 426 (brown dotted line)
 531 and INTA- Hornillos (purple solid line). Viscosity and temperature in function of time of analysis are showed. **B) Biplot**
 532 **from the principal component analysis for the six quinoa grain genotypes** using the pasting properties variables as
 533 input. The percentage of variance associate to each principal component is between parentheses. CHEN 426 (red),
 534 CHEN 252 (purple), CHEN 426 (black), CHEN 435 (green), CHEN 182 (blue), INTA-Hornillos (grey)

535

536



A**B**



Highlights

- The genetic diversity in the physicochemical and pasting properties was evaluated.
- Quinoa NWA genotypes are valuable for food and industrial applications.
- Highland genotypes showed stable viscosities and low breakdown values
- PCA lead to a good clustering of genotypes depending on their ecogeographic origin.

Journal Pre-proof

CONFLICT OF INTEREST

All authors declare that there is no conflict of interest.

Journal Pre-proof